PAPER

Synergy of adsorption and photosensitization of graphene oxide for improved removal of organic pollutants†

Chaobi Li,[a] Qiao Xu,[a] Shuxia Xu,[a] Xinfeng Zhang,*[a] Xiandeng Hou[b] and Peng Wu*[b]

Due to the various functional oxygen-containing groups, graphene oxide (GO) has been frequently explored as sorbent for various metal ions and organic pollutants. However, the adsorption capacity of solely GO is limited. Therefore, compositing GO with other adsorbents to improve the adsorption capacity is often required. On the other hand, the oxygen functional groups enable GO for exciton generation, which has been harvested for photosensitized generation of reactive oxygen species (ROS). Photosensitization has been explored for advanced pollutant degradation. Here, the adsorption and photosensitization effect of GO was synergized for improving the pollutant removal performance. Hydroquinone (HQ) was taken as the model pollutant for the illustration of the synergic effect. GO could adsorb HQ, possibly due to $\pi-\pi$ stacking and hydrogen-bonding interactions between GO and HQ. In the presence of white light irradiation (LED), the removal efficiency for HQ was greatly improved. Spectroscopic study indicated the improved removal efficiency could be ascribed to light irradiation-induced HQ oxidation. Further study showed that violet LEDs exhibited higher oxidation efficiency than white, blue, green, yellow, and red LEDs, since violet LEDs possess the largest spectra overlap with the absorption of GO. *Via* scavenger studies, the exact oxidants were identified as $^{\bullet}OH$, $^{1}O_2$, and $^{\bullet}O_2^{-}$, which are generated from GO photosensitization. Another intriguing feature is that GO can be recycled in several runs of adsorption/photosensitization of pollutants. Moreover, the synergic adsorption/photosensitization feature of GO can be extended to remove a broad band of phenolic pollutants, demonstrating the universality of such strategy for improved pollutant removal.

Introduction

Graphene oxide (GO) is a single-layer of graphite oxide and is usually produced by the chemical treatment of graphite through oxidation.[1] In contrast to graphene, the oxygenated lattice of GO provides good solubility and dispersibility in many solvents (particularly in water),[2] which received great interest in many areas such as optical biosensors[3] and diagnostics/therapeutic applications.[4] The availability of several types of oxygen-containing functional groups on the basal plane and the sheet edge allows GO to interact with a wide range of organic and inorganic materials in a non-covalent or ionic manner, leading to the adsorption of a variety of heavy metal ions and organic pollutants.[5] However, GO alone is not a highly efficient adsorbent. To increase the adsorption capacity and operability, compositing

of GO with other adsorbents, such as Fe_3O_4,[6] polymers,[7] and SiO_2,[8] is often used.

Photosensitization is a reaction that is mediated by light-absorbing substance, leading to the generation of reactive oxygen species (ROS) through the reduction of molecular oxygen by electron transfer (Type-I) as well as excitation of molecular oxygen by energy transfer (Type-II).[9] In photosensitized reactions, the absorbed photon excites the sensitizer to one or more energy-rich state(s). The excited sensitizer undergoes internal reactions that ultimately result in the chemical alteration of the oxygen. In Type-I reaction, the excited sensitizer reacts directly with oxygen, in a one-electron transfer reaction, to produce hydroxyl radical ($^{\bullet}OH$), superoxide radical anion ($^{\bullet}O_2^{-}$), and also hydrogen peroxide (H_2O_2). In Type-II reaction, the excited sensitizer transfers its excess energy to ground-state molecular oxygen, producing excited state singlet oxygen ($^{1}O_2$). These ROS feature great promise in environmental remediation (*e.g.*, water disinfection,[10] and degradation of pesticides,[11]) and photodynamic therapy (PDT).[9] Due to the luminescent property of GO,[12] ROS can also be generated from photosensitized GO.[13] Particularly, the broad absorption band of GO also facilitate combined PDT and photothermal therapy effects for the destruction of melanoma tumors in mice using ultra-low doses of NIR light.[14] However,

[a]College of Materials and Chemistry & Chemical Engineering, Chengdu University of Technology, Chengdu 610059, China. E-mail: zhangxinfeng09@cdut.cn

[b]Analytical & Testing Center, Sichuan University, Chengdu 610064, China. E-mail: wupeng@scu.edu.cn
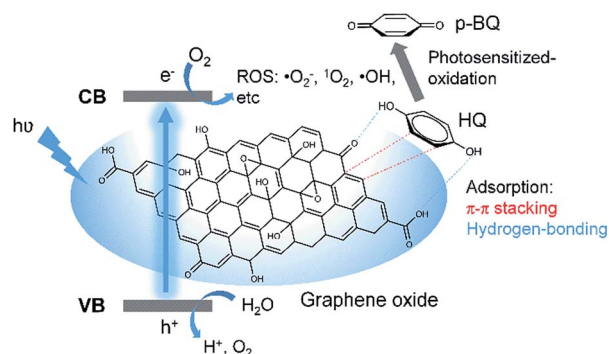
Scheme 1 Schematic illustration of the synergy of adsorption and photosensitized oxidation of GO for improved pollutants removal.

such promising photosensitization property has seldom been explored in pollutants removal.

In this work, therefore, GO was explored as both adsorbent and photosensitizer for pollutant removal. As shown in Scheme 1, pollutants bearing benzene and oxygen-containing moieties (here hydroquinone as the example) can be adsorbed by GO through possible π–π stacking and hydrogen bonding. In the presence of light irradiation, photosensitized GO generates ROS through an electrical pathway between its valence and conduction bands under an excitation state. The adsorbed pollutants can therefore be photo-oxidized *in situ*, leading to improved pollutants removal. Excitingly, since GO possess broad band absorption, the photosensitization can be achieved in the presence of white light irradiation.

Results and discussion

Photo-assisted removal of HQ by GO

Commercially-available GO was used as received. To illustrate the effect of adsorption and photosensitization of GO, hydroquinone (HQ) was taken as the model pollutant here. As shown in Fig. 1,
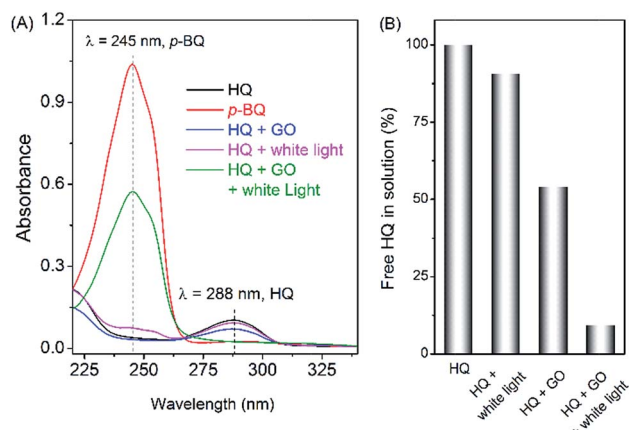
HQ has a characteristic absorbance band centered at 288 nm. Upon mixing of HQ with GO, the absorbance of the 288 nm-band decreased by about 40%, implying adsorption of HQ by GO. Interestingly, when irradiating the mixture of GO and HQ with a white LED for 30 min, the absorption band of HQ almost disappeared, giving rise to a new absorption peak at 245 nm. Such new peak matches perfectly with the characteristic absorbance of *p*-benzoquinone (*p*-BQ), the oxidation product of HQ. However, without white LED light irradiation, no clear sign of *p*-BQ was observed (Fig. 1A). These phenomena indicates that HQ is converted to *p*-BQ in the presence of GO and light irradiation. Control experiments showed that no significant light-induced oxidation of HQ (less than 10%) was observed in the absence of GO (Fig. 1B). Also, the light-induced oxidation of HQ could be significantly inhibited by removal of dissolved oxygen (bubbling with N_2). Therefore, the above experimental results indicated that the removing of HQ is the result of combined action of adsorption and photosensitized oxidation of GO.

Adsorption of HQ by GO

Firstly, the adsorption kinetics of HQ on GO was investigated at 298 K. As shown in Fig. 2A, the adsorption of HQ by GO increased quickly during the initial 30 min and then gradually levelled off upon further increasing the adsorption time, with equilibrium time of about 60 min and adsorption capacity of about 20 mg g^{-1}. The time dependence for the adsorption is better fitted by the pseudo-second-order model over pseudo-first-order model (Fig. 2B *versus* S1 and Table S1†), indicating that chemisorption is the rate-controlling step during the adsorption. Probably, the initial fast adsorption is due to the special single sheet structure and oxygenated lattice of GO that
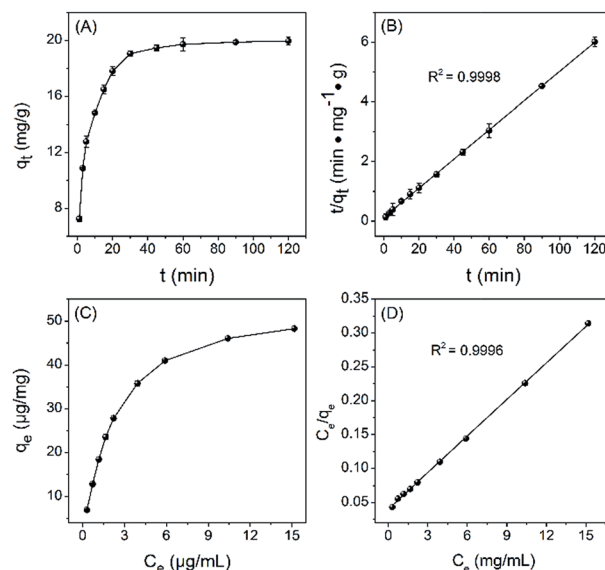

Fig. 1 Photo-assisted removal of HQ (2.5 mg L^{-1}) by GO (0.1 mg mL^{-1}): (A) UV-vis absorption spectra of HQ, *p*-BQ, HQ + GO, HQ + white light, and HQ + GO + white light; and (B) the residue free HQ upon interaction with white light, GO, and white light plus GO.

Fig. 2 Adsorption performance of GO for HQ: (A) the time-dependent absorption of HQ (2.5 mg L^{-1}) by GO (0.1 mg mL^{-1}); (B) fitting curve of the adsorption kinetics with pseudo-second-order model; (C) adsorption isotherm for HQ by GO at 298 K; and (D) fitting curve of the adsorption isotherm with Langmuir model.
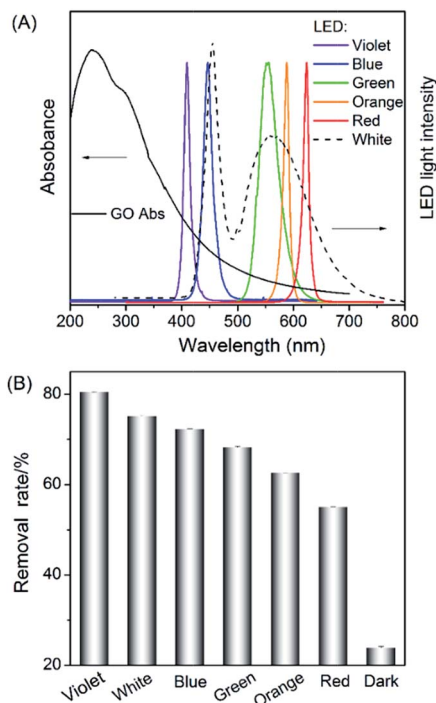
Fig. 3 Re-confirmation of the photosensitized oxidation of HQ: (A) the spectra overlap between the absorption spectrum of GO and lighting wavelength of various LEDs; and (B) the removal rate of HQ by GO assisted by violet, white, blue, green, orange, and red LED illumination for 10 min and under dark condition. Experiments were carried out with 0.1 mg mL^{-1} GO and 2.5 mg L^{-1} HQ.

can interact with HQ through possible π–π stacking and hydrogen-bonding (Scheme 1).

The adsorption thermodynamics, including standard free energy change (ΔG_0), enthalpy change (ΔH_0) and entropy change (ΔS_0), was determined from the temperature-dependent relationship of HQ adsorption by GO. As shown in Fig. S2,† the equilibrium adsorption capacity of HQ increases with increasing the temperature from 288 to 318 K, indicating that the adsorption of HQ is an endothermic process, which agrees well with the negative ΔG_0 (Table S2†). Considering both positive ΔH_0 and ΔS_0 (Table S2†), the driving force for HQ adsorption by GO may be controlled by an entropy effect rather enthalpy change.

The adsorption isotherms of HQ by GO were given in Fig. 2C. For better understanding the adsorption patterns, Langmuir and Freundlich equations were employed to simulate the adsorption isotherms (ESI†). The Langmuir model assumes that adsorption occurs on a homogeneous surface by monolayer coverage and no subsequent interaction between adsorbed species, while the Freundlich model is an empirical model based on multilayer adsorption on heterogeneous surfaces. As can be seen from Fig. 2D and Table S3,† Langmuir adsorption model was better to simulate the adsorption over Freundlich model, indicating that HQ adsorption by GO resulted in a monolayer coverage of HQ on the GO nanosheet. The maximum adsorption capacity (q_{max}) for the removal of HQ by GO obtained from the adsorption isotherms was 54.8 mg g^{-1} (Table S3†).

Photosensitized oxidation of HQ by GO

Photosensitized oxidation occurs first by photon absorption to trigger the transition from the ground state to the excited state. Therefore, the photosensitization efficiency is directly related to the light absorption. Here, we used LED (3 V, 3 W) as the lighting source for the photosensitization. As shown in Fig. 3A, GO exhibits a broad band absorption ranging from UV to visible region,[3a] resulting in the overlap between the GO absorption and LED lighting wavelength in the following order: violet > white > blue > green > orange > red. Just as expected, the HQ removal efficiency (photosensitization efficiency) was in good accordance with the above spectra overlap order (Fig. 3B). Namely, violet LED gave the best HQ removal performance among the LEDs used here. To simulate the sun light-induced photosensitization, here we chose white LED for irradiation. Without light illumination (dark), the HQ removal rate was quite low, further confirming the advantage of photosensitization in pollutant removal.

Upon light absorption, GO can proceed typical exciton process of typical semiconductors to emit red fluorescence.[12,15] Principally, the photosensitized oxidation of HQ by GO will accompany with the perturbation of the exciton process and thus reduced fluorescence. Just as expected, the introduction of HQ to the GO solution could gradually quench the fluorescence of GO (Fig. 4A) as well as the fluorescence lifetime (Fig. S3†).
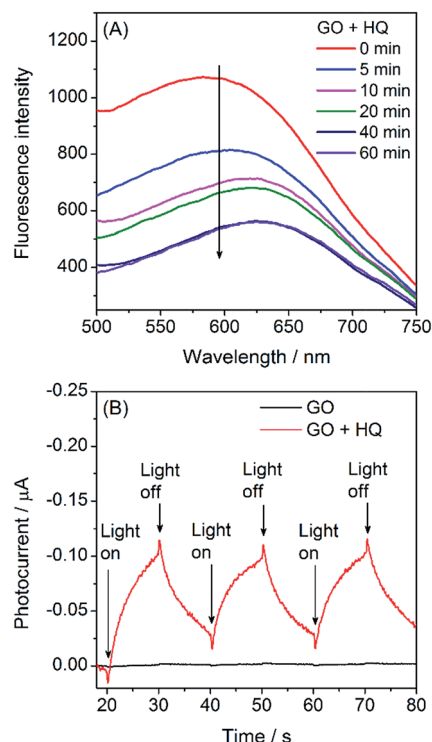

Fig. 4 Conformation of the exciton perturbation of GO by HQ: (A) time-dependent fluorescence quenching of GO (λ_{ex} = 350 nm) in the presence of HQ (2.5 mg L^{-1}); and (B) photocurrent response (i–t curve) of GO/ITO electrode in the absence and presence of HQ (25 mg L^{-1}). The photoelectrochemical tests were performed in 0.10 M PBS at a working potential of 0.0 V and white LED irradiation.[16]

Besides, the time-course of the fluorescence quenching is very similar to the adsorption kinetics HQ on GO (Fig. 2A). Meanwhile, we also used photoelectrochemistry to characterize this exciton process (ESI†). As shown in Fig. 4B, no appreciable photocurrent generation was observed in GO/ITO photoelectrode. However, cathodic photocurrent was observed when introduction of HQ to the electrolyte solution. Therefore, the fluorescence and photocurrent investigations confirmed that the photo-generated electrons did involve in the photosensitized oxidation of HQ.

Photosensitization can generate reaction oxygen species (ROS) through the reduction of molecular oxygen by electron transfer (Type-I) as well as energy transfer from the photoexcited GO (Type-II).[9] To analyze the role of O_2 in the photo-assisted pollutant removal, the removal performance of GO for HQ was compared under normal (air), oxygen-depleted (N_2 bubbling) and oxygen-enriched (O_2 bubbling) conditions. As shown in Fig. 5A, the removal rate was highest in oxygen-enriched solution and lowest in oxygen-depleted solution, which indicates the critical role of O_2 in photo-assisted HQ removal.

The light-assisted removal of pollutant is attributed to the photosensitized generation of ROS, such as $^1O_2$, $\cdot OH$, $\cdot O_2^-$, and H_2O_2. To uncover the role of specific ROS, we used the ROS-specific scavengers to evaluate the contribution of these ROS, namely mannite for $\cdot OH$, tryptophan for $^1O_2$, superoxide dismutase (SOD) for $\cdot O_2^-$, and catalase for H_2O_2.[17] As shown in Fig. 5B, the presence of mannite, tryptophan sand SOD shows inhibitory efficacy on HQ removal, while catalase cannot. Increasing the concentrations of mannite and tryptophan could further result in decreased HQ removal (Fig. S4†). These results imply that $\cdot OH$, $^1O_2$, and $\cdot O_2^-$ are the main ROS species toward HQ removal. Besides, we also used ethanolamine (TEOA) as a hole scavenger to reduce the electron–hole recombination of GO. The presence of TEOA could enhance the HQ removal (Fig. 5B and S4†), suggesting that TEOA should promote electrons in the conduction band of GO to generate more ROS. Such result is in good agreement with the photoelectrochemical investigations (Fig. 4B). Therefore, all the above investigations confirmed the role of photosensitization in photo-assisted HQ removal by GO.
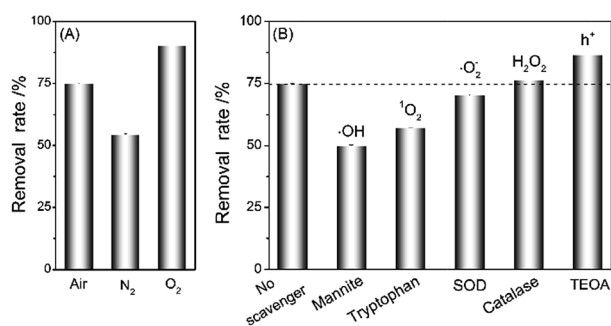
Factors that affect the synergic adsorption and photosensitization of pollutants

To maximize the synergic adsorption and photosensitization effects for pollutants, a series of factors were studied and optimized, including the media pH, the concentration of GO, and illumination time. As shown in Fig. S5A,† the removal rate significantly increased with the illumination time and the equilibrium was reached within 60 min. The optimal dosage of GO suspension used in this work is about 0.1 mg mL^{-1} (Fig. S5B†). The surface chemistry of GO and the removing of HQ were both highly dependent on the pH of the sample solution. The optimal pH of this system was 7.0 (Fig. S5C†).

Re-usability of GO for synergy of adsorption and photosensitization in pollutant removal

For practical use of such synergic effect of adsorption and photosensitization for pollutant removal, the re-usability of GO is very important from the economical point of view. Experimentally, we first demonstrated that the adsorbed p-BQ (the oxidation production of HQ) by GO could be simply eluted by water washing. Therefore, the GO after release of p-BQ could be explored for adsorption and photosensitized oxidation of HQ again (ESI†). As shown in Fig. 6, such process of adsorption/photosensitization-elution could be cycled, but the removal rate decreased from 95% to about 75% after 5 cycles. After detailed studying, we found the absorption characteristics of GO were retained before and after adsorption (Fig. S6†). Besides, morphological investigations with TEM indicated that no appreciable structural change of the GO nanosheet was observed before and after adsorption (Fig. S7†). The decreased pollutant removal performance was in fact due to the loss of GO rather than the loss of adsorption/photosensitization activity during the removal-elution run (Fig. 6 and S8†). Possibly, the relatively inert structure of GO is not destructed during cycling of adsorption/photosensitization. Such feature demonstrated that upon introduction of light-irradiation for photosensitized-oxidation, GO could be beneficial for cyclic removal of pollutants.

Universality of GO for synergic adsorption and photosensitization of pollutants

After demonstration of the success of synergic adsorption and photosensitization of GO for improved HQ removal, we next
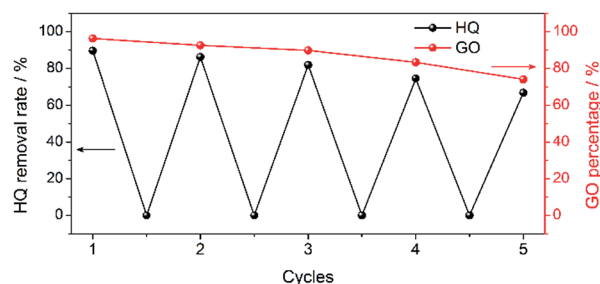

Fig. 5 Confirmation of the photosensitized generation of ROS for HQ removal: (A) effect of O_2-depletion and O_2-enriched GO solution for photo-assisted HQ removal; and (B) the use of scavenger for evaluation of the specific ROS in HQ removal. All samples were illuminated with white LED for 10 min.

Fig. 6 Cycling performance (adsorption/photosensitization-elution) of GO (0.1 mg L^{-1}) for removal of HQ (2.5 mg L^{-1}).
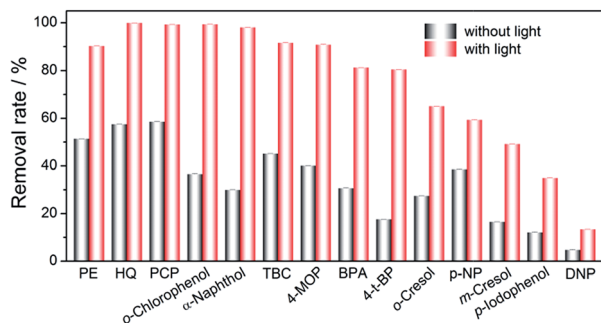
Fig. 7 Phenolic pollutant removal performance of GO in the absence and presence of white LED irradiation. GO concentration, 0.1 mg mL^{-1}; pollutant concentration, 1 μg mL^{-1}. PE, phenol; PCP, *p*-chlorophenol; TBC, 4-*tert*-butylcatechol; 4-MOP, 4-methoxyphenol; BPA, bisphenol A; 4-*t*-BP, *p-tert*-butylphenol, NP, *p*-nitrophenol; DNP, 2,4-dinitrophenol.

investigated the universality of this strategy for a broad band of pollutants. It is expected that the π system of GO provides good adsorption for contaminants containing benzene ring. Therefore, a series of phenolic contaminants, including phenol (PE), *p*-chlorophenol (PCP), *o*-chlorophenol, α-naphthol, 4-*tert*-butylcatechol (TBC), 4-methoxyphenol (4-MOP), bisphenol A (BPA), *p-tert*-butylphenol (4-*t*-BP), *o*-cresol, *p*-nitrophenol (NP), *m*-cresol, *p*-iodophenol, and 2,4-dinitrophenol (DNP), were subjected to GO adsorption and photosensitization. As shown in Fig. 7, all these phenolic contaminants could be adsorbed by GO. In the presence of white LED irradiation, the removal rate for all these pollutants could be largely increased. Compared with other sorbents for removal of phenolic contaminants,[18] the adsorption capacity of GO may be lower, but the photosensitization property endows GO further added removal rate for these contaminants. Besides, such removal can be cycled. Therefore, the synergic adsorption and photosensitization feature of GO can be explored for broad band pollutants removal.

The pollutant removal performance of GO in real-world sample matrix was further investigated. As shown in Table S4,† in tap water, lake water, and river water matrix, the removal rates for 0.5 mg L^{-1} of PE, HQ, and PCP are still higher than 95%. The promising performance on removal of phenolic pollutants shows great potential of GO as synergic adsorbent and photosensitizer for the visible-light oxidation of organic compounds in wastewater.

Conclusions

In summary, the photosensitization property of GO was firstly combined with its adsorption for improved pollutant removal. As the sorbent, GO exhibited medium adsorption capacity for phenolic pollutants. In the presence of light irradiation, the removal rates for these pollutants can be considerably improved, due to GO-involved *in situ* photosensitized oxidation. Such synergy of adsorption and photosensitized oxidation is universal in removal of a broad band of phenolic pollutants. Besides, due to the relatively inert structure, the photosensitized oxidation does not result in appreciable structure destruction of GO.

Therefore, GO can be re-cycled for adsorption/photosensitized oxidation of pollutants. Considering the laminar structure and available functionalization sites of GO, further conjugation of highly effective and stable photosensitizer with GO is expected to be promising in pollutant removal and water disinfection.

Acknowledgements

Notes and references

1 (*a*) D. Chen, H. B. Feng and J. H. Li, *Chem. Rev.*, 2012, **112**, 6027; (*b*) W. Y. Zhang, Y. X. Li, X. P. Zeng and S. Q. Peng, *Sci. Rep.*, 2015, **5**, 10589; (*c*) W. Y. Zhang, Y. X. Li, S. Q. Peng and X. Cai, *Beilstein J. Nanotechnol.*, 2014, **5**, 801.
2 D. R. Dreyer, S. Park, C. W. Bielawski and R. S. Ruoff, *Chem. Soc. Rev.*, 2010, **39**, 228.
3 (*a*) K. P. Loh, Q. L. Bao, G. Eda and M. Chhowalla, *Nat. Chem.*, 2010, **2**, 1015; (*b*) E. Morales-Narváez and A. Merkoçi, *Adv. Mater.*, 2012, **24**, 3298.
4 (*a*) L. Y. Feng, L. Wu and X. G. Qu, *Adv. Mater.*, 2013, **25**, 168; (*b*) L. H. Tang, Y. Wang and J. H. Li, *Chem. Soc. Rev.*, 2015, **44**, 6954.
5 (*a*) J. Bai, H. M. Sun, X. J. Yin, X. Q. Yin, S. S. Wang, A. E. Creamer, L. J. Xu, Z. Qin, F. He and B. Gao, *ACS Appl. Mater. Interfaces*, 2016, **8**, 25289; (*b*) K. Yang, B. Chen, X. Zhu and B. Xing, *Environ. Sci. Technol.*, 2016, **50**, 11066; (*c*) D. Robati, B. Mirza, M. Rajabi, O. Moradi, I. Tyagi, S. Agarwal and V. K. Gupta, *Chem. Eng. J.*, 2016, **284**, 687.
6 (*a*) D. L. Zhao, X. Gao, C. N. Wu, R. Xie, S. J. Feng and C. L. Chen, *Appl. Surf. Sci.*, 2016, **384**, 1; (*b*) G. Q. Xie, P. X. Xi, H. Y. Liu, F. J. Chen, L. Huang, Y. J. Shi, F. P. Hou, Z. Z. Zeng, C. W. Shao and J. Wang, *J. Mater. Chem.*, 2012, **22**, 1033; (*c*) Z. G. Geng, Y. Lin, X. X. Yu, Q. H. Shen, L. Ma, Z. Y. Li, N. Pan and X. P. Wang, *J. Mater. Chem.*, 2012, **22**, 3527.
7 L. C. Chen, S. Lei, M. Z. Wang, J. Yang and X. W. Ge, *Chin. Chem. Lett.*, 2016, **27**, 511.
8 (*a*) L. N. Yang, J. G. Hu, W. W. Wu, J. Tang, K. X. Ding and J. Li, *Chem. Eng. J.*, 2016, **306**, 77; (*b*) Y. Liu, X. G. Meng, Z. C. Liu, M. J. Meng, F. P. Jiang, M. Luo, L. Ni, J. Qiu, F. F. Liu and G. X. Zhong, *Langmuir*, 2015, **31**, 8841.
9 (*a*) H. Abrahamse and M. R. Hamblin, *Biochem. J.*, 2016, **473**, 347; (*b*) S. S. Lucky, K. C. Soo and Y. Zhang, *Chem. Rev.*, 2015, **115**, 1990.
10 C. Liu, D. Kong, P.-C. Hsu, H. Yuan, H.-W. Lee, Y. Liu, H. Wang, S. Wang, K. Yan, D. Lin, P. A. Maraccini, K. M. Parker, A. B. Boehm and Y. Cui, *Nat. Nanotechnol.*, 2016, **11**, 1098.
11 (*a*) M. Nowakowska, M. Sterzel, S. Zapotoczny and E. Kot, *Appl. Catal., B*, 2005, **57**, 1; (*b*) J. P. Escalada, A. Pajares, J. Gianotti, A. Biasutti, S. Criado, P. Molina, W. Massad,

F. Amat-Guerri and N. A. García, *J. Hazard. Mater.*, 2011, **186**, 466.

12 (*a*) X. M. Sun, Z. Liu, K. Welsher, J. T. Robinson, A. Goodwin, S. Zaric and H. J. Dai, *Nano Res.*, 2008, **1**, 203; (*b*) J. L. Chen, X. P. Yan, K. Meng and S. F. Wang, *Anal. Chem.*, 2011, **83**, 8787.

13 (*a*) T. Dutta, R. Sarkar, B. Pakhira, S. Ghosh, R. Sarkar, A. Barui and S. Sarkar, *RSC Adv.*, 2015, **5**, 80192; (*b*) Y. X. Wang, Y. B. Xie, H. Q. Sun, J. D. Xiao, H. B. Cao and S. B. Wang, *ACS Appl. Mater. Interfaces*, 2016, **8**, 9710.

14 P. Kalluru, R. Vankayala, C. S. Chiang and K. C. Hwang, *Biomaterials*, 2016, **95**, 1.

15 Z. T. Luo, P. M. Vora, E. J. Mele, A. T. C. Johnson and J. M. Kikkawa, *Appl. Phys. Lett.*, 2009, **94**, 111909.

16 P. Wu, J.-B. Pan, X.-L. Li, X. D. Hou, J.-J. Xu and H.-Y. Chen, *Chem.–Eur. J.*, 2015, **21**, 5129.

17 (*a*) Y. J. Chung, B. I. Lee, J. W. Ko and C. B. Park, *Adv. Healthcare Mater.*, 2016, **5**, 1560; (*b*) E. G. Ju, K. Dong, Z. W. Chen, Z. Liu, C. Q. Liu, Y. Y. Huang, Z. Z. Wang, F. Pu, J. S. Ren and X. G. Qu, *Angew. Chem., Int. Ed.*, 2016, **55**, 11467.

18 (*a*) U. Soni, J. Bajpai, S. K. Singh and A. K. Bajpai, *J. Water Process Eng.*, 2017, **16**, 56; (*b*) H. M. Abd El Salam, S. A. Younis, H. R. Ali and T. Zaki, *Microporous Mesoporous Mater.*, 2017, **241**, 210; (*c*) B. Kakavandi, M. Jahangiri-rad, M. Rafiee, A. R. Esfahani and A. A. Babaei, *Microporous Mesoporous Mater.*, 2016, **231**, 192.